# Rotational Doppler effect in x-ray photoionization

Yu-Ping Sun,[1,2,*] Chuan-Kui Wang,[1,2] and Faris Gel'mukhanov[2,†]
[1]*College of Physics and Electronics, Shandong Normal University, 250014 Jinan, China*
[2]*Theoretical Chemistry, Roslagstullsbacken 15, Royal Institute of Technology, S-106 91 Stockholm, Sweden*
(Received 23 March 2010; published 10 November 2010)

The energy of the photoelectron experiences a red or blue Doppler shift when the molecule recedes from the detector or approaches him. This results in a broadening of the photoelectron line due to the translational thermal motion. However, the molecules also have rotational degrees of freedom and we show that the translational Doppler effect has its rotational counterpart. This rotational Doppler effect leads to an additional broadening of the spectral line of the same magnitude as the Doppler broadening caused by translational thermal motion. The rotational Doppler broadening as well as the rotational recoil broadening is sensitive to the molecular orbital from which the photoelectron is ejected. This broadening should be taken into account in analysis of x-ray photoemission spectra of super-high resolution and it can be directly observed using x-ray pump-probe spectroscopy.

DOI: 10.1103/PhysRevA.82.052506 PACS number(s): 33.15.Mt, 33.20.Rm, 33.80.Eh, 33.70.Jg

## I. INTRODUCTION

Due to significant resolution improvements of x-ray photoemission (XPE) spectroscopy the spectral line broadening becomes a key question. Very often one can see nicely separated vibrational progression of the XPE band. We discuss here the spectral shape of certain vibrational components of the XPE profile. The main mechanisms of the broadening in gas phase measurements are the natural line broadening caused by the finite lifetime of the ionized state, the translational Doppler, and the instrumental broadenings [1,2]. The role of the translational Doppler broadening caused by the photoelectron momentum increases with increasing photoelectron energy or temperature.

When the momentum of the photoelectron is high one can also see the line shift and broadening caused by the excitation of the rotational levels due to the rotational recoil effect [3–6]. Similar to the Doppler effect the recoil effect is one of the fundamental physical phenomena, which was extensively studied in nonlinear laser spectroscopy in optical and IR regions [7,8]. Different aspects of the recoil effect in the photoelectron and Auger spectroscopies were explored in articles [9–13]. In x-ray photoemission both translational recoil and translational Doppler effects are the consequence of the momentum conservation law and are related to the momentum of the ejected photoelectron.

The momentum of the photoelectron is large in the case of x-ray photoionization of the valence shell. Because of this the translational Doppler broadening is much larger than the lifetime broadening of the final ionic state. This makes the translational Doppler broadening one of the most important effects for photoelectron spectroscopy of high resolution. A conventional experimental technique to suppress the translational Doppler effect is cooling molecules to low temperature by supersonic expansion [2,5]. It should be noted that the translational Doppler effect can be anomalously enhanced in the case of resonant x-ray photoemission from molecules with dissociative core-excited state [14–17].

According to classical mechanics there exists very close analogy between translational and rotational degrees of freedom [18]: momentum-angular momentum, velocity-angular velocity, translational recoil effect-rotational recoil effect. This succession suggests that one should expect a rotational analog for the translational Doppler effect. The main aim of our study is to show that, indeed, the rotational Doppler effect exists and the related broadening is of the same order of magnitude as the translational Doppler broadening. In spite of this similarity the manifestation of the rotational Doppler effect is rather different to the translational counterpart. Both translational and rotational Doppler effects are essentially classical notions. For instance, a single vibrational line cannot be shifted due to the translational Doppler effect related to the bound nuclear motion. However, the center of gravity of the XPE band is Doppler shifted if the number of vibrational lines in the XPE profile is large [17]. Similarly, the rotational Doppler effect is an adequate concept only in classical limit when the angular momentum $J$ is high enough.

This paper is organized as follows. In the next section (Sec. II) we outline the theory of the rotational Doppler effect. To make the theory complete the translational Doppler and recoil effects are also included in our analysis. Section III is devoted to discussions of the obtained results. Our findings are summarized in the last section, Sec. IV.

## II. THEORY

In this work we concentrate the analysis on the x-ray photoemission of the electron from the molecular orbital (MO) $\psi$. The photoionization happens if the photon energy $\omega_{\rm ph}$ is larger than the ionization potential ($V_{\rm ion}$) of this MO. When the molecule is irradiated by x rays, both the momentum $\mathbf{k}$ and the kinetic energy $E = k^2/2 = \omega_{\rm ph} - V_{\rm ion}$ of the photoelectron are large due to high value of $\omega_{\rm ph}$. Because of the thermal motion the molecule has velocity $\mathbf{v}$. This results in a translational Doppler shift of the XPE resonance [19],

$$\mathbf{k} \cdot \mathbf{v}, \tag{1}$$

*yuping@theochem.kth.se
†On leave from Institute of Automation and Electrometry, 630090 Novosibirsk, Russia.

 

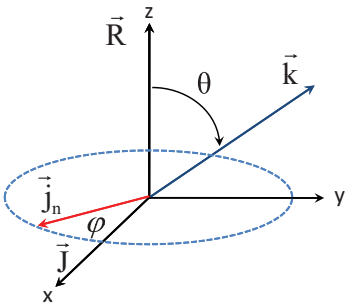


FIG. 1. (Color online) The frame of integration.

and a related translational Doppler broadening. However, the molecule also rotates when the temperature $T$ is not equal to zero. A strong analogy between translational and rotational degrees of freedom exists. Every physical quantity for translational motion has a rotational equivalent. For example, mass $M$, momentum of inertia $I$; velocity $\mathbf{v}$, angular velocity $\boldsymbol{\omega}$; momentum $\mathbf{k}$, angular momentum $\mathbf{j} = [\mathbf{R} \times \mathbf{k}]$, where $\mathbf{R} = \mathbf{R}_1 - \mathbf{R}_2$ is the internuclear radius vector. This means that one can expect the translational Doppler shift (1) to have its rotational counterpart,

$$\mathbf{j} \cdot \boldsymbol{\omega}. \tag{2}$$

Let us now show that this naive expectation is indeed true.

### A. Amplitude of the photoionization

The molecular orbital of diatomic molecule $A_1A_2$,

$$\psi = c_1\psi_1 + c_2\psi_2, \tag{3}$$

is the linear combination of the atomic orbitals (AO) $\psi_1$ and $\psi_2$ localized on the atoms $A_1$ and $A_2$, respectively. To treat correctly the rotational degrees of freedom, the origin of the frame should be in the center of gravity of the molecule. The atoms $A_1$ and $A_2$ have the coordinates $\mathbf{R}_1 = \alpha_1\mathbf{R}$ and $\mathbf{R}_2 = -\alpha_2\mathbf{R}$ in this frame, respectively. Here $\alpha_1 = m_2/M$, $\alpha_2 = m_1/M$ where $m_n$ is the mass of the $n$th atom and $M = m_1 + m_2$.

The matrix element of the photoionization reads in the high-energy approximation,

$$\langle\psi|\mathbf{e}\cdot\mathbf{r}|\psi_{\mathbf{k}}^-\rangle \propto d_1 e^{\imath\alpha_1\mathbf{k}\cdot\mathbf{R}} + d_2 e^{-\imath\alpha_2\mathbf{k}\cdot\mathbf{R}}. \tag{4}$$

We use atomic units. To avoid cumbersome theory let us assume that the AO $\psi_n$ is the $s$-atomic orbital, and hence $d_n \propto c_n(\mathbf{e}\cdot\mathbf{k})$. Here $\mathbf{e}$ is the polarization vector of x rays. According to Eq. (4) the amplitude of the rotational transition $JM \to J'M'$ in the course of x-ray ionization,

$$F = F_1 + F_2, \tag{5}$$

is the sum of the partial ionization amplitudes for each atom [3,13]:

$$F_n = \frac{d_n\langle JM|e^{\pm\imath\alpha_n\mathbf{k}\cdot\mathbf{R}}|J'M'\rangle\sqrt{\Gamma}}{\Delta E - \mathbf{k}\cdot\mathbf{v} + \frac{k^2}{2M} + E_{J'} - E_J + \imath\Gamma}. \tag{6}$$

Here $\Delta E = E - (\omega_{\rm ph} - V_{\rm ion})$. $\Gamma$ is the lifetime broadening of the final ionic state. $E_J = J(J+1)/2I$ and $E_{J'} = J'(J'+1)/2I$ are rotational energies of the ground $|JM\rangle = Y_{JM}$ and final $|J'M'\rangle = Y_{J'M'}$ rotational states, respectively. $I = \mu R^2$ is the momentum of inertia and $\mu = m_1m_2/M$ is the reduced mass of the molecule. The signs + and − correspond to $n = 1$ and 2, respectively. The absolute square of the ionization amplitude results in the Fermi golden rule for the cross section which takes maximum at the resonance $\Delta E = \mathbf{k}\cdot\mathbf{v} - \frac{k^2}{2M} - E_{J'} + E_J$. The momentum exchange between the photoelectron and the molecule results in a shift of the XPE resonance due to the Doppler ($\mathbf{k}\cdot\mathbf{v}$) and the recoil ($\Delta_{\rm tr} = k^2/2M$) effects caused by the translational motion. One should notice that we study here the transitions only to the bound nuclear states which have narrow resonances.

### B. Cross section of the photoionization in classical limit

The ionization cross section $|F_1 + F_2|^2 = |F_1|^2 + |F_2|^2 + 2\mathrm{Re}(F_1^*F_2)$ is the sum of three contributions. In x-ray photoemission the de Broglie wavelength of the photoelectron exceeds significantly the internuclear distance $R$,

$$kR \gg 1, \tag{7}$$

starting from soft-x-ray region $E \gtrsim 100$ eV. Due to this the interference term $2\mathrm{Re}\,(F_1^*F_2)$ can be neglected because it is suppressed by the factor $1/(kR) \ll 1$ in comparison with the cross section of ionization $|F_n|^2$ of the $n$th atom [13,16,20]:

$$\sigma \approx \sigma_1 + \sigma_2. \tag{8}$$

To get the partial cross section $\sigma_n$, the squared scattering amplitude $|F_n|^2$ should be convoluted with the Boltzmann velocity distribution $W(\mathbf{v}) = \exp(-\mathbf{v}^2/\bar{v}^2)/(\sqrt{\pi}\,\bar{v})^3$ and summed over initial and final rotational states,

$$\begin{aligned}\sigma_n &= \int d\mathbf{v}W(\mathbf{v}) \sum_{JM,J'M'} \rho(J)|F_n|^2 \\ &= \Gamma d_n^2 \int d\mathbf{v}W(\mathbf{v}) \sum_{JM,J'M'} \rho(J) \\ &\quad\times \frac{\langle JM|e^{\pm\imath\alpha_n\mathbf{k}\cdot\mathbf{R}}|J'M'\rangle\langle J'M'|e^{\mp\imath\alpha_n\mathbf{k}\cdot\mathbf{R}}|JM\rangle}{\left(\Delta E - \mathbf{k}\cdot\mathbf{v} + \frac{k^2}{2M} + E_{J'} - E_J\right)^2 + \Gamma^2},\end{aligned} \tag{9}$$

where $\bar{v} = \sqrt{2k_BT/M}$ is the thermal velocity and $k_B$ is the Boltzmann constant.

The thermal Doppler broadening in the high-energy region prevents resolving the rotational structure in the XPE spectra. Furthermore it should be noted that rather high rotational levels of many diatomic molecules are populated already for room temperature ($J \sim \sqrt{2Ik_BT} \sim 10$).

$$J \gg 1. \tag{10}$$

The molecule experiences additional rotational heating in the course of the photoionization because of the large recoil angular momentum ($\sim kR \gg 1$). This allows us to use the classical limit for rotational degrees of freedom. The rotational distribution $\rho(J)$ of the ground state is normalized to one, $\sum_{JM}\rho(J) = \sum_J(2J+1)\rho(J) = 1$. In the classical limit (10), $\rho(J)$ has the following form:

$$\rho(J) \approx \frac{1}{2Ik_BT}\exp\left(-\frac{J^2}{2Ik_BT}\right) = \frac{1}{I^2\overline{\omega}^2}e^{-\omega^2/\overline{\omega}^2}, \tag{11}$$

where $\overline{\omega} = \sqrt{2k_BT/I}$ is the thermal angular velocity. The rotational energy $E_J \approx J^2/2I = I\omega^2/2$ is expressed through the classical angular velocity $\boldsymbol{\omega} = \mathbf{J}/I$ of the molecule in the ground state.

Let us rewrite the cross section (9) in the time domain:

$$\sigma_n = d_n^2 \mathrm{Re} \int d\mathbf{v} W(\mathbf{v}) \int_0^\infty dt e^{\imath(\Delta E - \mathbf{k}\cdot\mathbf{v} + \frac{k^2}{2M} + \imath\Gamma)t} \times \sum_{JM} \rho(J) \langle JM | e^{\pm\imath\alpha_n \mathbf{k}\cdot\mathbf{R}} e^{\mp\imath\alpha_n \mathbf{k}\cdot\mathbf{R}(t)} | JM \rangle, \quad (12)$$

using $\frac{\Gamma}{x^2+\Gamma^2} = \mathrm{Re}\int_0^\infty dt e^{\imath(x+\imath\Gamma)t}$ and the operator identity $\hat{B} f(\hat{A}) \hat{B}^{-1} = f(\hat{B}\hat{A}\hat{B}^{-1})$. The operator,

$$\mathbf{R}(t) = e^{\imath H_{\mathrm{rot}} t} \mathbf{R} e^{-\imath H_{\mathrm{rot}} t}, \quad (13)$$

obeys the Heisenberg equation $\dot{\mathbf{R}} = \imath[H_{\mathrm{rot}}, \mathbf{R}] = [-\mathbf{R} \times \hat{\mathbf{J}} + \hat{\mathbf{J}} \times \mathbf{R}]/2I$, in which the rotational Hamiltonian $H_{\mathrm{rot}} = \hat{\mathbf{J}}^2/2I$ is expressed in terms of the operator of angular momentum $\hat{\mathbf{J}} = -\imath \hat{\mathbf{R}} \times \boldsymbol{\nabla}$.

The cross section (12) is written in the framework of strict quantum theory. We will now come to the actual approximations to get the semiclassical limit for rotational degrees of freedom. The formal solution (13) is too cumbersome. However, both translational and rotational Doppler effects result in the broadening $D$, which is much larger than the spacing between rotational levels because of high energy of the photoelectron. Due to this the dephasing caused by the Doppler effect quenches the large time contribution ($t > 1/D$) in the XPE cross section [see Eq. (19)]. The fact that the dephasing happens much faster than the molecular rotations ($1/D\tau_{\mathrm{rot}} \sim 1/kR \ll 1$) allows us to simplify the strict solution (13) by truncating the Taylor expansion of $\exp(\pm\imath H_{\mathrm{rot}} t)$ to the first order:

$$\mathbf{R}(t) \approx \mathbf{R} + \imath t[H_{\mathrm{rot}}, \mathbf{R}] = \mathbf{R} + \frac{t}{2I}[-\mathbf{R} \times \hat{\mathbf{J}} + \hat{\mathbf{J}} \times \mathbf{R}], \quad t \lesssim \frac{1}{D} \ll \tau_{\mathrm{rot}} \sim \omega^{-1}. \quad (14)$$

Our objective now is to extract the rotational operator from $e^{\mp\imath\alpha_n \mathbf{k}\cdot\mathbf{R}(t)}$ in Eq. (12) and move it to the right-hand side where it acts directly on the state $|JM\rangle$ with the well-defined value of the classical angular momentum $|\mathbf{J}|$. The corresponding derivation is outlined in semiclassical limit (7), (10) in Appendix. According to Eq. (A9),

$$e^{\pm\imath\alpha_n \mathbf{k}\cdot\mathbf{R}} e^{\mp\imath\alpha_n \mathbf{k}\cdot\mathbf{R}(t)} \approx e^{\imath j_n^2 t/2I} e^{-\frac{\imath}{I}\mathbf{j}_n\cdot\hat{\mathbf{J}}}. \quad (15)$$

As was mentioned at the beginning of Sec. II, the angular momentum $[\mathbf{R} \times \mathbf{k}]$ should be responsible for the excitation of rotations by the ejected photoelectron contrary to the translational momentum $\mathbf{k}$ which affects the translational motion. Now we can see the explicit rotational counterpart of $\mathbf{k}$. This is the recoil angular momentum,

$$\mathbf{j}_n = \pm\alpha_n[\mathbf{R} \times \mathbf{k}], \quad j_n = \alpha_n kR \sin\theta, \quad (16)$$

which the molecule gets in the course of the ejection of electron from the $n$th atom. Here $\theta = \angle(\mathbf{R}, \mathbf{k})$. The recoil angular momentum, in an agreement with intuition, depends on the mass of the atom which emits the electron and it has an opposite direction for atoms 1 and 2.

A key element in semiclassical approximation (15) is to apply the Heisenberg's correspondence principle [21] to the rotational operator,

$$e^{-\frac{\imath}{I}\mathbf{j}_n\cdot\hat{\mathbf{J}}} \to e^{-\frac{\imath}{I}\mathbf{j}_n\cdot\mathbf{J}} = e^{-\imath\mathbf{j}_n\cdot\boldsymbol{\omega}t}, \quad (17)$$

where the vector $\mathbf{J} = I\boldsymbol{\omega}$ is the classical angular momentum ($|\mathbf{J}| = J + 1/2 \approx J$). Taking into account Eqs. (15) and (17) and

$$\sum_M |Y_{JM}(\theta,\varphi)|^2 = \frac{2J+1}{4\pi} \approx \frac{J}{2\pi}, \quad (18)$$

we get

$$\sigma_n = \frac{d_n^2}{2\pi} \mathrm{Re} \int d\mathbf{v} W(\mathbf{v}) \int_0^\infty dt e^{\imath(\Delta E - \mathbf{k}\cdot\mathbf{v} + \frac{k^2}{2M} + \imath\Gamma)t} \times \int d\Omega_{\mathbf{R}} \sum_J J\rho(J) e^{\imath(-\mathbf{j}_n\cdot\boldsymbol{\omega} + j_n^2/2I)t}, \quad (19)$$

where $d\Omega_{\mathbf{R}}$ is the solid angle of $\mathbf{R}$.

Evidently the integration over orientations of the molecular axis $\mathbf{R}$ with fixed $\mathbf{k}$ can be replaced by the integration over orientations of $\mathbf{k}$ with fixed $\mathbf{R}$: $d\Omega_{\mathbf{R}} = d\Omega_{\mathbf{k}}$. Both vectors $\boldsymbol{\omega}$ and $\mathbf{j_n}$ are lying in the plane orthogonal to $\mathbf{R}$. Due to this the solid angle $d\Omega_{\mathbf{k}}$ can be replaced by $\sin\theta d\theta d\varphi$, where $\varphi = \angle(\boldsymbol{\omega}, \mathbf{j}_n)$ is nothing else than the azimuthal angle of $\mathbf{k}$ (see Fig. 1). The integration of the right-hand side of Eq. (19) is straightforward:

$$\sigma_n = \frac{\Gamma d_n^2}{2\pi\overline{\omega}^2} \int d\mathbf{v} W(\mathbf{v}) \int_0^\pi \sin\theta d\theta \int_0^{2\pi} d\varphi \int_0^\infty d\omega\omega \times \frac{\exp\left(-\frac{\omega^2}{\overline{\omega}^2}\right)}{\left(\Delta E - \mathbf{k}\cdot\mathbf{v} + \frac{k^2}{2M} - \mathbf{j}_n\cdot\boldsymbol{\omega} + \frac{j_n^2}{2I}\right)^2 + \Gamma^2}. \quad (20)$$

The physical reason for the two-dimensional (2D) rotational Boltzmann distribution at the right-hand side of Eq. (20) is that the linear molecule has two orthogonal rotations $\boldsymbol{\omega} = (\omega_1, \omega_2)$,

$$\exp\left(-\frac{\omega^2}{\overline{\omega}^2}\right) d\varphi\omega d\omega = \exp\left(-\frac{\omega_1^2 + \omega_2^2}{\overline{\omega}^2}\right) d\omega_1 d\omega_2. \quad (21)$$

Let us now decrease the number of the integrals in Eq. (20). The 2D rotational Boltzmann distribution is reduced to a one-dimensional (1D) one when we orient $\omega_1$ along $\mathbf{j}_n$. It should be noted that both vectors $\boldsymbol{\omega}$ and $\mathbf{j}_n$ lie in the plane perpendicular to the molecular axis $\mathbf{R}$. Similarly, the three-dimensional (3D) velocity distribution $W(\mathbf{v}) = W(v_x)W(v_y)W(v_z)$ is reduced to the 1D distribution $W(v_z) = \exp(-v_z^2/\bar{v}^2)/\sqrt{\pi}\bar{v}$ if $v_z$ is oriented along $\mathbf{k}$. Therefore,

$$\sigma_n = \frac{\Gamma d_n^2}{2\pi\overline{\omega}\bar{v}} \int_0^\pi d\theta \sin\theta \int_{-\infty}^\infty d\omega \int_{-\infty}^\infty dv \times \frac{\exp\left(-\frac{\omega^2}{\overline{\omega}^2} - \frac{v^2}{\bar{v}^2}\right)}{\left(\Delta E - kv + \frac{k^2}{2M} - j_n\omega + \frac{j_n^2}{2I}\right)^2 + \Gamma^2}. \quad (22)$$

Here the superscripts in $\omega_1$ and $v_z$ are omitted. Note that the recoil angular momentum $j_n$ depends on $\theta$ according to

Eq. (16). The auxiliary variables,

$$\zeta = kv + j_n\omega, \quad \eta = -j_n v + k\omega, \tag{23}$$

results in a great simplification of the integral at the right-hand side of Eq. (22). Indeed, taking into account that $dvd\omega = d\zeta d\eta/(k^2 + j_n^2)$ we obtain

$$\sigma_n = \frac{\Gamma d_n^2}{2\sqrt{\pi}} \int_0^\pi d\theta \frac{\sin\theta}{D_n(\theta)} \int_{-\infty}^{\infty} d\zeta \frac{\exp\left(-\frac{\zeta^2}{D_n^2(\theta)}\right)}{\left(\Delta E + \Delta_n(\theta) - \zeta\right)^2 + \Gamma^2}, \tag{24}$$

where the total shift of the resonance,

$$\Delta_n(\theta) = \Delta_{\rm tr} + \Delta_{\rm rot}^{(n)}(\theta), \quad \Delta_{\rm tr} = \frac{k^2}{2M},$$
$$\Delta_{\rm rot}^{(n)}(\theta) = \frac{j_n^2}{2I} = \frac{\alpha_n^2 k^2 R^2}{2I}\sin^2\theta, \tag{25}$$

is the sum of the shifts caused by translational and rotational recoil effects, respectively. The total Doppler broadening,

$$D_n(\theta) = \sqrt{D_{\rm tr}^2 + D_{\rm rot}^{(n)2}(\theta)} = \sqrt{k^2\bar{v}^2 + j_n^2\bar{\omega}^2}, \tag{26}$$

includes both the translational Doppler broadening $D_{\rm tr} = k\bar{v}$ and the rotational one $D_{\rm rot}^{(n)}(\theta) = j_n\bar{\omega} = \alpha_n kR\bar{\omega}\sin\theta$. The rotational Doppler broadening contrary to the translational Doppler effect depends on the atom from which the electron is ejected. For example,

$$D_{\rm rot}^{(1)}(\theta) = D_{\rm tr}\sqrt{\frac{m_2}{m_1}}\sin\theta. \tag{27}$$

This expression says that the ejection of electron from the light atom results in a larger rotational Doppler broadening.

It is useful to also write down the expression for the ionization cross section in the classical limit:

$$\sigma = \frac{1}{2}\int d\Omega_{\mathbf{R}} \int d\mathbf{v} W(\mathbf{v}) \int d\boldsymbol{\omega} W(\boldsymbol{\omega}) |F|^2,$$
$$F = F_1 + F_2, \tag{28}$$
$$F_n \approx \sqrt{\Gamma}\frac{d_n e^{\pm\imath\alpha_n \mathbf{k}\cdot\mathbf{R}}}{\Delta E - \mathbf{k}\cdot\mathbf{v} + k^2/2M - \mathbf{j}_n\cdot\boldsymbol{\omega} + j_n^2/2I + \imath\Gamma},$$

which results in Eqs. (8) and (20). Here $W(\boldsymbol{\omega}) = W(\omega_1)W(\omega_2) = e^{-\boldsymbol{\omega}^2/\bar{\omega}^2}/\pi\bar{\omega}^2$ is the rotational Boltzmann distribution.

### C. Ionization of the valence shell

Let us now consider an important case of the valence shell ionization. In this case the final ionic state with a hole in the valence shell has a long lifetime from about 1 ns to 1 ps. The Lorentzian at the right-hand side of Eq. (24) can be replaced by the $\delta$ function, because $\Gamma \ll D_n$. The resulting cross section is a simple expectation value of the Gaussian,

$$\sigma_n = \frac{d_n^2\sqrt{\pi}}{2}\int_0^\pi d\theta \frac{\sin\theta}{D_n(\theta)} \exp\left(-\frac{[\Delta E + \Delta_n(\theta)]^2}{D_n^2(\theta)}\right), \quad \Gamma \ll D_n. \tag{29}$$

## III. DISCUSSION

To illustrate the theory let us consider the single vibrational peak of the gas phase carbon monoxide molecule (for example, in the $X\,^2\Sigma^+$ XPE band). We will analyze here only the partial cross section $\sigma_C$ related to the carbon contribution ($n = C$). The results for $\sigma_O$ are very similar because the factor $\sqrt{m_O/m_C}$ is close to one. Figure 2 shows the spectral shapes for different energies of the photoelectron. When the energy of the photoelectron $E$ is rather low [Fig. 2(a)], both the shift and the broadening of the XPE line are relatively small. The extra broadening of the line is mainly caused by the rotational Doppler effect, which is very close to the translational Doppler broadening ($D_{\rm tr} = 0.053$ eV, $D_{\rm rot} = \sqrt{D^2 - D_{\rm tr}^2} = 0.047$ eV). The deviation of $D_{\rm rot}$ from $D_{\rm tr}$ is mainly due to the mass factor $\sqrt{m_O/m_C} \approx 1.15$ and $\sin\theta \approx \sqrt{\overline{\sin^2\theta}} \approx \sqrt{2/3}$ [see Eq. (27)]. Both the translational Doppler broadening (TDB) and the rotational Doppler broadening (RDB) grow as $\sqrt{E}$ when the photoelectron energy increases. The XPE line experiences an additional broadening because of the rotational recoil effect when $E$ is high enough. This is the reason why $D_{\rm rot}$ and $D_{\rm tr}$ are almost the same and equal to 0.13 eV at $E = 3$ keV [Fig. 2(b)]. Here one can see also the asymmetry of the

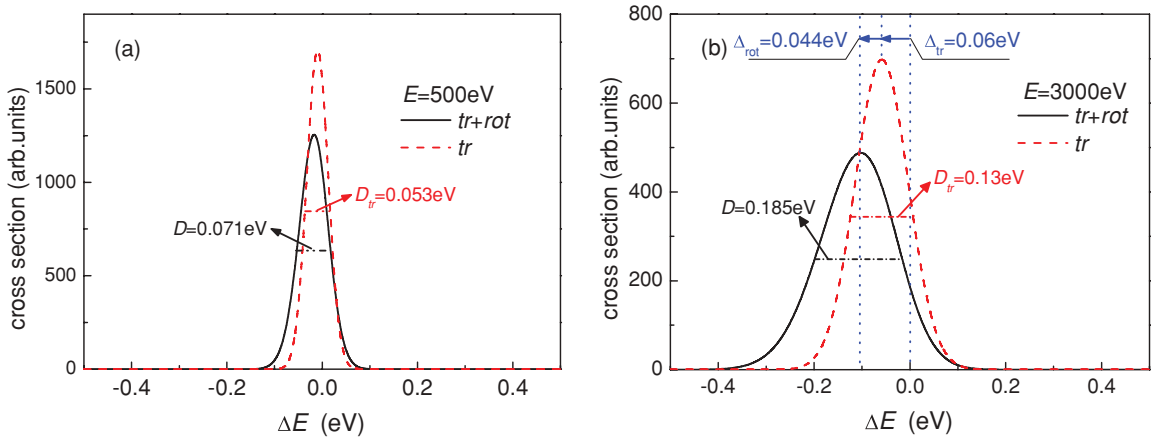


FIG. 2. (Color online) The spectral shape of the single vibrational line of the CO molecule (29). The dashed line shows the profile calculated without taking into account the rotational degrees of freedom [$\alpha_n = 0$ in Eq. (29)] in contrast to the solid line which shows the cross section where all degrees of freedom are taken into account.

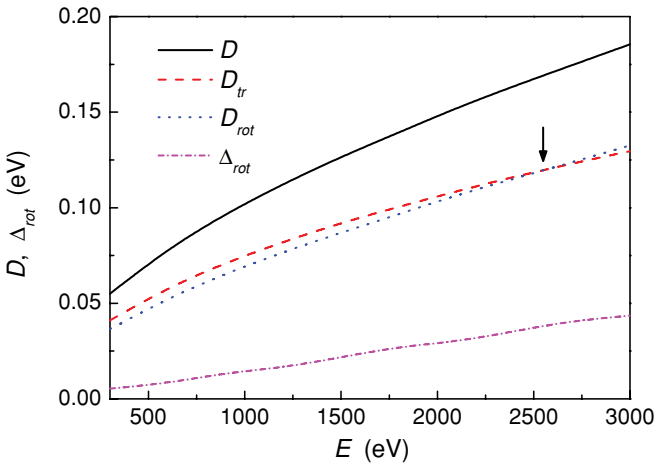


FIG. 3. (Color online) The total ($D$), translation ($D_{\rm tr}$), and rotational ($D_{\rm rot}$) broadenings and the shift $\Delta_{\rm rot}$ of the XPE line caused by the rotational recoil effect. Here the broadening $D$ is the full width at half maximum (FWHM) contrary to Eq. (29). The arrow shows the point ($E \approx 2.5$ keV) where $D_{\rm tr} = D_{\rm rot}$. Calculations are based on Eq. (29).

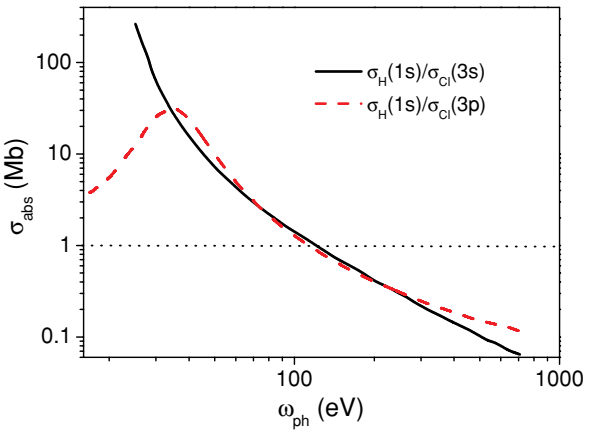


FIG. 4. (Color online) The ratios $\sigma_H(1s)/\sigma_{\rm Cl}(3s)$ and $\sigma_H(1s)/\sigma_{\rm Cl}(3p)$ of the photoionization cross sections (per electron) of the hydrogen and chlorine atoms versus the photon energy $\omega_{\rm ph}$ (calculations are based on the data from Ref. [25]).

line caused by the rotational recoil effect. The reason for this asymmetry is the angular dependence of the rotational recoil shift $\Delta_{\rm rot}(\theta) = j_n^2/2I \propto \sin^2\theta$. To avoid cumbersome notations we skip here and below the index $n$: $\Delta_{\rm rot}^{(n)} \to \Delta_{\rm rot}$, $D_{\rm rot}^{(n)} \to D_{\rm rot}$.

The translational recoil effect shifts the XPE line by $\Delta_{\rm tr} = k^2/2M = 60$ meV. The shift caused by the rotational recoil effect is slightly smaller, $\Delta_{\rm rot} = 44$ meV. This value of $\Delta_{\rm rot}$ is in a reasonable agreement with the simple estimation $\Delta_{\rm rot} \approx \overline{\Delta_{\rm rot}(\theta)} = \Delta_{\rm tr} 2m_O/3m_C = 54$ meV. Here the overline means the orientational averaging.

Figure 3 displays the energy dependence of the total broadening (D), partial contributions $D_{\rm tr}$, $D_{\rm rot}$, and the rotational shift $\Delta_{\rm rot}$. One can see that the rotational Doppler broadening is slightly smaller than the translational one. An additional broadening caused by the rotational recoil effect makes $D_{\rm rot}$ larger than $D_{\rm tr}$ starting from $E \approx 2.5$ keV.

A few words about the possibility for experimental observation of the rotational Doppler effect. The main difficulty is that this broadening usually occurs simultaneously with the translation Doppler effect.

(1) The RDB can be extracted from the experimental data by measuring the slope of the broadening versus photon energy.

(2) One can also suppress or enhance the rotational Doppler effect in comparison with the translational one. This is the case when the recoil angular momentum $j_n$ is small or large. According to Eq. (27) one can expect a significant increase of the RDB if the molecule has a light atom. Let us consider the photoionization of the $5\sigma$ and $2\pi$ electrons of the HCl molecule with the adiabatic binding energy about 17 and 13 eV, respectively [22–24]. Both ionized states $A(^2\Sigma^+)$ and $X(^2\Pi_i)$ are bound [22,23]. The highest occupied molecular orbital (MO) $2\pi$ consists of mainly $3p_\pi$ atomic orbitals of the Cl atom. Consequently, the $X(^2\Pi_i)$ band corresponds to ejection of the photoelectron from the Cl atom, $\sigma \approx \sigma_{\rm Cl}$. The molecular orbital $5\sigma \approx C_{3p}3p_\sigma^{\rm Cl} + C_{3s}3s^{\rm Cl} + C_{1s}1s^H$ is chosen because it has a large contribution of the $1s$ function of hydrogen. The ionization cross section is a sum of the contributions from light (H) and heavy (Cl) atoms (8), $\sigma = \sigma_H + \sigma_{\rm Cl}$. The relative photoionization cross sections per one electron $\sigma_H(1s)/\sigma_{\rm Cl}(3p)$ and $\sigma_H(1s)/\sigma_{\rm Cl}(3s)$ (Fig. 4) show that the probabilities of the ejections of the electron from hydrogen and chlorine atoms are comparable in the energy region 100 eV$\lesssim E \lesssim$ 200 eV. The RDB is larger for $\sigma_H$ than for $\sigma_{\rm Cl}$ because $j_H = j_{\rm Cl}m_{\rm Cl}/m_H \gg j_{\rm Cl}$. Due to this the total Doppler broadening $D^H$ for the hydrogen atom is very close to the rotational Doppler broadening $D_{\rm rot}^H \approx D_{\rm tr}\sqrt{2m_{\rm Cl}/3m_H}$. For example, $D^H$ [full width at half maximum (FWHM)] is equal to 103 and 147 meV for $E = 100$ and 200 eV, respectively. These values are about 5 times larger than the corresponding translational Doppler broadenings $D_{\rm tr}$(FWHM) $\approx 20$ and 30 meV. Here, for example, $D_{\rm tr}$(FWHM) $= 2\sqrt{\ln 2}D_{\rm tr}$.

The RDB for the ionization channel related to the Cl atom is suppressed by the factor $m_H/m_{\rm Cl} \approx 0.03$ in comparison with the hydrogen atom, because the Doppler broadening related to this ionization channel is very close to small translational Doppler broadening $D_{\rm tr}$.

Since the total cross section (8) is the sum of the partial cross sections $\sigma = \sigma_H + \sigma_{\rm Cl}$, one can expect the narrow peak [with FWHM about 20 (30) meV for $E = 100$ (200) eV] related to the ionization of the chlorine atom and broad pedestal [with FWHM about 103 (147) meV for $E = 100$ (200) eV] caused by ejection of the electron from the hydrogen. In contrast to the considered $5\sigma$ ionization channel, the broad RDB pedestal is absent in the case of photoionization of the $2\pi$ electron.

It is worth mentioning that the RDB can also be observed for the HF molecule, which is rather similar to HCl.

(3) One can decrease significantly the RDB in the case of nonlinear molecules like the nitride anion $NO_2^-$. The ultraviolet photoelectron spectrum of $NO_2^-(X\,^1A_1)$ has been studied by Ervin *et al.* [26]. This band is related to ionization of the $4a_1$ electron localized on the nitrogen atom (lone pair). This means that the rotation around the bisectrix of the angle ONO is not excited when the $4a_1$ electron is ejected. The estimation shows that the rotational broadening is smaller

(about 2/3) when the photoelectron is ejected from the nitrogen in comparison with the ionization of the oxygen atom. Let us note that contrary to the lone pair, other molecular orbitals also include atomic orbitals of the oxygen atoms. Thus, the comparison of the width of the single vibrational line of the final state $^1A_1$ with the broadening of the vibrational lines of other final electronic states gives a unique opportunity of direct experimental verification of the rotational Doppler effect.

(4) The rotational Doppler effect can be directly observed using the pump-probe experiment where strong IR laser rotationally accelerates jet-cooled molecules. The supersonic expansion suppresses strongly the TDB while the laser field results in rotational heating [27] up to $J \sim 100$ and hence, strong rotational Doppler broadening. The comparison of the XPE profiles with and without the laser field gives the desired rotational broadening. In principle, the pump radiation can rotate the molecule in a certain direction and it can induce the angular momentum with well-defined orientation. In this case the XPE line will be shifted due to the rotational Doppler effect.

## IV. SUMMARY

It is shown the x-ray photoelectron line is broadened due to the rotational Doppler effect which is the rotational counterpart of the translational Doppler effect. This extra broadening has the same magnitude as the translational Doppler broadening. Therefore this mechanism of the broadening of the spectral line should be taken into account in the analysis of the experimental x-ray photoelectron spectra. We show that the rotational Doppler effect in contrast to its translational counterpart is sensitive to the molecular orbital from which the photoelectron is ejected because it depends on mass of the atom which the photoelectron leaves. The reason for this is the angular recoil momentum which depends on the ionization site.

The rotational Doppler broadening can be measured for molecules with light atoms like HCl and HF where this broadening is significantly larger than the translational Doppler broadening. We predict a broad pedestal (about 100 meV) for the HCl molecule caused by the rotational Doppler effect. The width of this pedestal being about 100 meV in the soft-x-ray region grows as $\sqrt{E}$ when the energy of the photoelectron increases. The conventional synchrotron radiation light sources allow one to approach the energy region about 1 keV [6]. High brilliance of the x-ray free-electron laser (XFEL) [28,29] allows one to reach higher energies of the photoelectron where the rotational Doppler broadening is larger. We suggest an x-ray pump-probe experiment which would allow a direct measurement of the broadening caused by the rotational Doppler effect.

## ACKNOWLEDGMENTS

We acknowledge support from the Swedish Research Council (VR), Carl Tryggers Stiftelse (CTS) foundation, Swedish Institute (Visby Program), National Natural Science Foundation of China (Grant No. 10974121) and National Basic Research Program of China (Grant No. 2006CB806000).

## APPENDIX: CLASSICAL LIMIT

In this section we are going to outline the way how to handle the autocorrelation function,

$$\langle JM|e^{-\imath\alpha\mathbf{k}\cdot\mathbf{R}}e^{\imath\alpha\mathbf{k}\cdot\mathbf{R}(t)}|JM\rangle, \tag{A1}$$

in the semiclassical limit (7), (10). The short time approximation (14) for $\mathbf{R}(t)$ gives

$$e^{\imath\alpha\mathbf{k}\cdot\mathbf{R}(t)} = \exp\left\{\imath\alpha\mathbf{k}\cdot\mathbf{R} + \frac{\imath\alpha t}{2I}(-\mathbf{k}\cdot[\mathbf{R}\times\hat{\mathbf{J}}] + \mathbf{k}\cdot[\hat{\mathbf{J}}\times\mathbf{R}])\right\}.$$

The main idea of the derivation is to extract the rotational operator from this expression and move it to the right-hand side. Here the rotational operator will act directly on the eigen function of the momentum $Y_{JM}$ with a well-defined value of the classical angular momentum $|\mathbf{J}| \approx J + 1/2$. To proceed further we use the Baker-Campbell-Hausdorff formula,

$$e^{\imath\alpha\mathbf{k}\cdot\mathbf{R}(t)} = e^{A+B} = e^A e^B e^{-\frac{1}{2}[A,B]} e^{\frac{1}{3}(2[B,[A,B]]+[A,[A,B]])}\ldots. \tag{A2}$$

First, we need the commutator,

$$[A,B] = \frac{\alpha^2 t}{2I}\{[(\mathbf{k}\cdot\mathbf{R}),\mathbf{k}\cdot[\mathbf{R}\times\hat{\mathbf{J}}]] - [(\mathbf{k}\cdot\mathbf{R}),\mathbf{k}\cdot[\hat{\mathbf{J}}\times\mathbf{R}]]\}, \tag{A3}$$

of the operators,

$$A = \imath\alpha\mathbf{k}\cdot\mathbf{R}, \quad B = \frac{\imath\alpha t}{2I}(-\mathbf{k}\cdot[\mathbf{R}\times\hat{\mathbf{J}}] + \mathbf{k}\cdot[\hat{\mathbf{J}}\times\mathbf{R}]). \tag{A4}$$

The properties of antisymmetric tensor $\varepsilon_{ikl}$ and the formulas,

$$[\hat{J}_i, R_j] = \imath\sum_k \varepsilon_{ijk}R_k, \quad \sum_{ij}\varepsilon_{ijk}\varepsilon_{ijt} = 2\delta_{kt},$$
$$\sum_i \varepsilon_{imn}\varepsilon_{ikl} = (\delta_{mk}\delta_{nl} - \delta_{ml}\delta_{nk}), \tag{A5}$$

yield

$$[(\mathbf{k}\cdot\mathbf{R}),\mathbf{k}\cdot[\mathbf{R}\times\hat{\mathbf{J}}]] = -[(\mathbf{k}\cdot\mathbf{R}),\mathbf{k}\cdot[\hat{\mathbf{J}}\times\mathbf{R}]] = -\imath|\mathbf{k}\times\mathbf{R}|^2. \tag{A6}$$

The substitution of this expression at the right-hand side of Eq. (A3) gives

$$[A,B] = -\imath\frac{\alpha^2 t}{I}|\mathbf{k}\times\mathbf{R}|^2 = -\imath\frac{\alpha^2 t}{I}k^2R^2\sin^2\theta. \tag{A7}$$

Turning to the Baker-Campbell-Hausdorff formula (A2), it will be useful only if the commutators with $A$ and $B$ are small. This is indeed the case. For example, the commutator,

$$[B,[A,B]] \sim \frac{\alpha^3 t^2}{I^2}k^3R^3 \sim \left(\frac{t}{I}k^2R^2\right)^2 \times \frac{1}{kR}$$
$$\ll t^2\Delta_{\rm tr}^2 \sim \frac{\Delta_{\rm tr}^2}{D^2} \ll 1, \tag{A8}$$

is much smaller than the squared ratio of the translational recoil energy $\Delta_{\rm tr} = k^2/2M$ to the Doppler broadening. The same reason allows us to permute $e^B$ and $e^{-\frac{1}{2}[A,B]}$. Thus $e^{A+B} \approx e^A e^B e^{-\frac{1}{2}[A,B]} \approx e^A e^{-\frac{1}{2}[A,B]} e^B$. The operator $e^B$ can

be simplified:

$$e^{B} = \exp\left[\frac{\imath\alpha t}{2I}(-2\mathbf{k}\cdot[\mathbf{R}\times\hat{\mathbf{J}}] + 2\mathbf{k}\cdot\mathbf{R})\right] \approx \exp\left[\frac{-\imath\alpha t}{I}(\mathbf{k}\cdot[\mathbf{R}\times\hat{\mathbf{J}}])\right],$$

since $\mathbf{k}\cdot[\mathbf{R}\times\hat{\mathbf{J}}] - \mathbf{k}\cdot[\hat{\mathbf{J}}\times\mathbf{R}] = 2[\mathbf{k}\cdot[\mathbf{R}\times\hat{\mathbf{J}}] - (\mathbf{k}\cdot\mathbf{R})]$ and because $J \gg 1$ [or $\frac{\alpha t}{2I}\mathbf{k}\cdot\mathbf{R} \sim \frac{\alpha t}{2I}k^2R^2 \times \frac{1}{kR} \ll \Delta_{\mathrm{tr}}t$]. Hence,

$$e^{\imath\alpha\mathbf{k}\cdot\mathbf{R}(t)} = e^{A+B} \approx e^{\imath\alpha\mathbf{k}\cdot\mathbf{R}}e^{\imath\frac{\alpha^2 t}{2I}|\mathbf{k}\times\mathbf{R}|^2}e^{\frac{-\imath\alpha t}{I}(\mathbf{k}\cdot[\mathbf{R}\times\hat{\mathbf{J}}])} = e^{\imath\alpha\mathbf{k}\cdot\mathbf{R}}e^{\imath\frac{\alpha^2 t}{2I}|\mathbf{k}\times\mathbf{R}|^2}e^{\frac{\imath\alpha t}{I}([\mathbf{R}\times\mathbf{k}]\cdot\hat{\mathbf{J}})}. \quad \text{(A9)}$$


[1] D. W. Turner, Proc. Roy. Soc. A **307**, 15 (1968).
[2] K. Siegbahn, Philos. Trans. R. Soc. London A **318**, 3 (1986).
[3] I. L. Thomas, Phys. Rev. A **4**, 457 (1971).
[4] W. Domcke and L. S. Cederbaum, J. Electron Spectrosc. Relat. Phenom. **13**, 161 (1978).
[5] H. C. Choi, R. M. Rao, A. G. Mihill, S. Kakar, E. D. Poliakoff, K. Wang, and V. McKoy, Phys. Rev. Lett. **72**, 44 (1994).
[6] T. D. Thomas *et al.*, Phys. Rev. A **79**, 022506 (2009).
[7] S. G. Rautian and A. M. Shalagin, *Kinetic Problems of Nonlinear Spectroscopy* (North-Holland, Amsterdam, 1991).
[8] W. Demtroder, *Laser Spectroscopy: Basic Concepts and Instrumentation* (Springer Verlag, Berlin-Heidelberg, 2002).
[9] E. D. Poliakoff, H. C. Choi, R. M. Rao, A. G. Mihill, S. Kakar, K. Wang, and V. McKoy, J. Chem. Phys. **103**, 1773 (1995).
[10] V. C. Felicissimo, F. F. Guimaraes, and F. Gel'mukhanov, Phys. Rev. A **72**, 023414 (2005).
[11] Y. Takata *et al.*, Phys. Rev. B **75**, 233404 (2007).
[12] S. K. Semenov *et al.*, J. Phys. B: At. Mol. Opt. Phys. **39**, L261 (2006).
[13] K. Ueda, X.-J. Liu, G. Prümper, T. Lischke, T. Tanaka, M. Hoshino, H. Tanaka, I. Minkov, V. Kimberg, and F. Gel'mukhanov, Chem. Phys. **329**, 329 (2006).
[14] F. Gel'mukhanov, H. Ågren, and P. Sałek, Phys. Rev. A **57**, 2511 (1998).
[15] O. Björneholm *et al.*, Phys. Rev. Lett. **84**, 2826 (2000).
[16] F. Gel'mukhanov and H. Ågren, Phys. Rep. **312**, 91 (1999).
[17] P. Sałek, F. Gel'mukhanov, T. Privalov, and H. Ågren, Chem. Phys. Lett. **328**, 425 (2000).
[18] H. Goldstein, *Classical Mechanics* (Addison-Wesley, Reading, 1980).
[19] D. Turner, C. Baker, and C. Brundle, *Molecular Photoelectron Spectroscopy* (Willey, New York, 1970).
[20] F. Gel'mukhanov and H. Ågren, Phys. Rev. A **49**, 4378 (1994).
[21] S. C. McFarlane, J. Phys. B: At. Mol. Opt. Phys. **27**, 1913 (1994).
[22] D. Edvardsson, P. Baltzer, L. Karlsson, M. Lundqvist, and B. Wannberg, J. Electron Spectrosc. Relat. Phenom. **73**, 105 (1995).
[23] A. J. Yencha, A. J. Cormack, R. J. Donovan, A. Hopkirk, and G. C. King, Chem. Phys. **238**, 109 (1998).
[24] F. Burmeister, Ph.D. thesis, Uppsala University, 2003.
[25] I. Lindau, in *X-Ray Data Booklet*, Sec. 1.5, Figs. 1–4 (Lawrence Berkeley National Laboratory, University of California, Berkeley, 2009) [http://xdb.lbl.gov].
[26] K. M. Ervin, J. Hoe, and W. C. Lineberger, J. Phys. Chem. **92**, 5405 (1988).
[27] D. M. Villeneuve, S. A. Aseyev, P. Dietrich, M. Spanner, M. Yu. Ivanov, and P. B. Corkum, Phys. Rev. Lett. **85**, 542 (2000).
[28] T. Tschentcher, Chem. Phys. **299**, 271 (2004).
[29] T. Shintake *et al.*, Nature Photonics **2**, 555 (2008).